

Available online at www.sciencedirect.com

journal homepage: www.elsevier.com/locate/issn/15375110

Research Paper

A parameterised model of maize stem cross-sectional morphology



Michael A. Ottesen ^a, Ryan A. Larson ^a, Christopher J. Stubbs ^b,
Douglas D. Cook ^{a,*}

^a Department of Mechanical Engineering, 350 Engineering Building, Provo, UT 84601, USA

^b School of Computer Sciences and Engineering, Fairleigh Dickinson University, 1000 River Rd, Teaneck, NJ, 07666, USA

ARTICLE INFO

Article history:

Received 30 April 2021

Received in revised form

9 March 2022

Accepted 21 March 2022

Published online 26 April 2022

Keywords:

maize

cross-section

model

morphology

parameterised/parameterized

sensitivity

Stalk lodging, or failure of the stalk structure, is a serious problem in the production of maize (corn). Addressing this problem requires an understanding of the parameters that influence lodging resistance. Computational modelling is a powerful tool for this purpose, but current modelling methods have limited throughput and do not provide the ability to modify individual geometric features. A parameterised model of the maize stalk has the potential to overcome these limitations. The purposes of this study were to (a) develop a parameterised model of the maize stalk cross-section that could accurately simulate the physical response of multiple loading cases, and (b) use this model to rigorously investigate the relationships between cross-sectional morphology and predictive model accuracy. Principal component analysis was utilised to reveal underlying geometric patterns which were used as parameters in a cross-sectional model. A series of approximated cross-sections was created that represented various levels of geometric fidelity. The true and approximated cross-sections were modelled in axial tension/compression, bending, transverse compression, and torsion. For each loading case, the predictive accuracy of each approximated model was calculated. A sensitivity study was also performed to quantify the influence of individual parameters. The simplest model, an elliptical cross-section consisting of just three parameters: major diameter, minor diameter, and rind thickness, accurately predicted the structural stiffness of all four loading cases. The modelling approach used in this study model can be used to parameterise the maize cross-section to any desired level of geometric fidelity, and could be applied to other plant species.

© 2022 IAgE. Published by Elsevier Ltd. All rights reserved.

1. Introduction

Crop losses due to stalk lodging (failure of the grain stalk) limit worldwide food production. For maize alone, these losses

average approximately 5% annually, resulting in considerable loss of revenue (Duvick, 2005; USDA, 2018). In the field, grain stalks experience complex dynamic loading. Stalks predominantly fail because bending loads cause localised Brazier

* Corresponding author.

E-mail address: ddc971@byu.edu (D.D. Cook).

<https://doi.org/10.1016/j.biosystemseng.2022.03.010>

1537-5110/© 2022 IAgE. Published by Elsevier Ltd. All rights reserved.

Nomenclature (in order of appearance within the text)

| | |
|------------------|--|
| CT | x-ray computed tomography |
| i | Index specifying angular location in degrees, $i = 1, 2, 3, \dots, 360$ |
| j | Principal component index, $j = 1, 2, 3, \dots, 360$ |
| k | Cross-section index, $k = 1, 2, 3, \dots, 12,740$ |
| N | Number of included principal components, $N = 1, 2, 3, \dots, 360$ |
| R_{ik} | True (non-approximated) radial values ($i = 1, 2, \dots, 360$) of cross-section k |
| e_{ik} | Radial values of an ellipse which has been fit to cross-section k |
| r_{ik} | Residuals obtained by subtracting radial ellipse fit values from true radial values |
| P_{ik} | Principal component terms |
| S_{jk} | Principal component scaling factors for cross-section k |
| ϵ_{ikN} | Radial error when using N principal components ($\epsilon_{ikN} = 0$ when $N = 360$) |
| a | Major diameter of an ellipse |
| b | Minor diameter of an ellipse |
| t | Rind thickness |
| K | Stiffness |
| E | Young's Modulus |
| A | Cross-sectional area |
| L | Length |
| G | Shear modulus |
| I | Area moment of inertia |
| J | Polar moment of inertia |
| F | Force |
| 8 | Displacement |
| S | Normalised sensitivity |
| x | Input parameter |
| y | Output parameter |

buckling (Robertson et al., 2015) Brazier buckling occurs when the cross-section ovalises to a critical point and then collapses (Schulgasser & Witztum, 1992).

There is a broad and well-established research literature on stalk lodging that has sought to address this problem from agronomic, biological, anatomical, breeding, and genetic approaches (Ahmad et al., 2018; Davis & Crane, 1976; Devey & Russell, 1983; Erndwein et al., 2020; Flint-Garcia et al., 2003; Gou et al., 2007; Hondroyianni et al., 2000; Ma et al., 2014; Manga-Robles et al., 2021; Sun et al., 2018; Willman et al., 1987; Zhang et al., 2014, 2019). In the past several years, new insights have emerged as analysis and modelling tools from the field of biomechanical engineering have been applied to stalk lodging. These approaches can be grouped into two main categories: measurement/analysis techniques, and modelling.

In terms of engineering analysis/measurement techniques, a forensic engineering failure analysis provided a description of the most common modes and physiological locations of maize stalk lodging (Robertson et al., 2015). New phenotyping methods have included a mobile wind machine (Wen et al., 2019), devices for measuring stalk bending strength (Cook et al., 2019; Gomez et al., 2017; Hu et al., 2013;

Sekhon et al., 2020), new rind puncture resistance techniques (Seegmiller et al., 2020; Stubbs, McMahan, et al., 2020) and the measurement of flexural deformation (Guo et al., 2019; Reneau et al., 2020, 2020; Tongdi et al., 2011).

Engineering models are another promising new avenue for increasing our understanding of stalk lodging. Engineering models are based upon physical laws and can range from relatively simple beam models to highly realistic computational representations of the stalk. Engineering models provide two advantages, first, they suggest relationship patterns that have not previously been explored, such as relationships between flexural stiffness and strength (Robertson, Lee, et al., 2016) or between section modulus and strength (Robertson et al., 2017). Second, these models can be used to investigate factors and effects that are impossible to control in an experiment. For example, fully parameterised models can be used to perform optimisation and sensitivity studies aimed at identifying the influence of individual features of the stalk on its strength.

The most commonly applied computational tool in this domain is the finite-element method. The first finite-element models of maize stalk examined bending stresses rather than structural failure (Von Forell et al., 2015). Forell et al. hypothesised that discrepancies between the influence of material properties and morphology could provide a new way to create stalks that were both robust and digestible into biofuel. An inverse finite-element approach has been used to obtain estimates of the transverse material properties of maize tissues (Stubbs et al., 2019). The first finite-element model of maize stalk failure refined several of the findings of the earlier study by Forell et al. (Stubbs et al., 2022) Both Forell et al. (2015) and Stubbs et al., (2022) noted a need for parameterised (i.e., controllable) models of maize stalk morphology. This is because specimen-specific models have two significant limitations. First, the process to create specimen-specific models often requires manual manipulations, making it very time-intensive. Second, once generated, the morphology of specimen-specific models cannot be manipulated, thus preventing essential optimisation and sensitivity studies. Parameterised models enable population-based studies that provide much more general results than specimen-specific studies (Cook et al., 2014; Weizbauer & Cook, 2022).

Parameterisation of the maize stalk geometry would remove these limitations, thus enabling population-based. In human biomechanics, this approach has been successfully used to create flexible, multi-purpose models of the human pelvis, femur, spine, uterus, and eye, among others (Besnault et al., 1998; Klein et al., 2015; Maurel et al., 1997; Sigal et al., 2010). In this study, we focused on parameterizing the transverse cross section of the maize stalk (longitudinal and transverse cross-sections are shown in Fig. 1). This approach was chosen because it provides a balance between computational cost and model complexity. In early research stages, simple models are preferred since they can be thoroughly investigated, enable large sample sizes, and thus enable global sensitivity analyses (Saltelli & Funtowicz, 2014). By beginning with simple models, the pitfalls associated with over-developed models can be avoided (Cook et al., 2014).

This study was designed to address several questions related to the construction of accurate yet efficient computational models. An ellipse was observed to effectively predict the bending strength of maize stalks (Robertson et al., 2017).

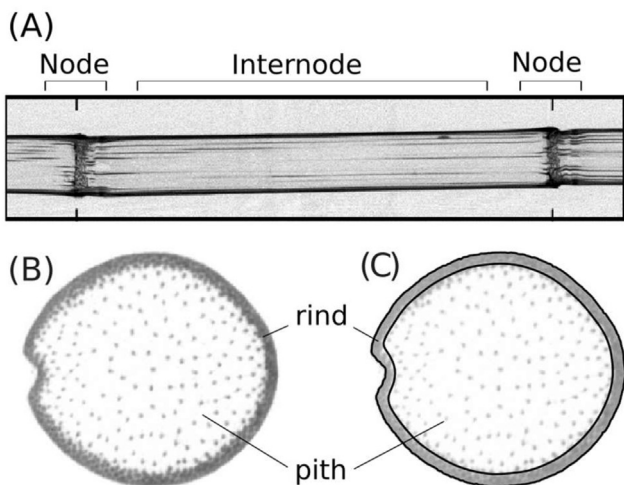


Fig. 1 – CT (Computed tomography) scan of maize stalks. A) longitudinal cross-section; B) transverse cross-section; C) the same transverse cross-section, showing segmentation boundaries between the rind and pith.

Questions posed included: Is the ellipse also effective in capturing the behaviour of maize stalks in other relevant loading situations such as torsion, axial tension/compression, and transverse compression? What degree of geometric detail is needed to capture the structural behaviour of the maize stalk in each of these loading scenarios? Can the shape of the maize stalk be parameterised such that essential features of the stalk can be controlled?

The purpose of this study was to answer these questions. To do this a parameterised model of the maize stalk cross-section was created. This model allowed the stalk geometry to be controlled (as opposed to previous studies which were observational in nature). The influence of geometry on model accuracy was then tested by varying the geometry in multiple ways while subjecting the geometric model to transverse, longitudinal, bending, and torsional loading cases. The use of multiple test cases and methods is known as triangulation and serves was used to increase the reliability of results (Lawlor et al., 2016; Nelson et al., 2019).

As a model-development study, the present research was not designed to study any specific factor influencing lodging or any specific grain varieties. Furthermore, this study does not account for all aspects of the true three-dimensional loading experienced by a maize stalk. Instead, this study was designed to provide essential new tools and information to be used in future modelling studies which will be able to more efficiently address such issues and questions. This information provided in this study will allow future researchers to select the appropriate level of modelling detail for the desired research objective.

2. Methods

2.1. Overview

This study involves a decomposition and parameterisation of the transverse cross-section of maize stalks as the first step

toward a fully three-dimensional parameterisation. The process involved geometric decomposition, which produced a method for creating approximations of a true maize cross-section at varying levels of fidelity. These different models were then assessed using three methods: purely geometric accuracy/error, mechanical response accuracy/error, and sensitivity to model parameters. The purpose of these assessments was to understand how varying levels of geometric fidelity influenced the corresponding structural response. When studying complex biological systems, it is important to incorporate adequate biological variation (Cook et al., 2014). Simple structural models were therefore intentionally chosen because they enabled the creation of thousands of unique models (as opposed to the less representative approach, which is to create highly complex models, but with a limited sample size).

2.2. Geometric decomposition and parameterisation

The goal of geometric analysis was to decompose the shape of the maize cross-section into controllable components of varying influence. Cross-sectional images were obtained from a database of maize stalk CT scans which was described in a previous study (Robertson et al., 2017). These stalks represented 5 commercial hybrids. To obtain high levels of geometric variation, each hybrid was grown at 5 different planting densities. This approach was used because planting density has a strong influence on stalk morphology and therefore increased the degree of geometric variation within the sample (Ma et al., 2014; Sher et al., 2017; Song et al., 2016). Edge-detection techniques were used to identify the interior and exterior boundaries of the rind region for each CT image (Robertson et al., 2017). A representative CT cross-section image of a maize stalk is shown in Fig. 1. Each stalk was rotated to match the orientation shown in the figure. Principal component decomposition was based on a polar (i.e. radial/tangential) coordinate system located at the geometric centre of each cross-section (see Fig. 2). A total of 360 circumferential sample points were sampled at regular circumferential intervals along the exterior surface of each cross-sectional image.

An initial attempt to decompose geometry using only principal component analysis had produced unfavourable results. A hybrid method produced much more useful results. The hybrid method combined least-squares regression with principal component analysis. In our prior research, we observed that a simple ellipse with a constant rind thickness provides an excellent approximation of maize stalk cross-sections (Robertson et al., 2017). Using this knowledge, an ellipse was fitted to the exterior boundary of each cross-section using a least-squares approach. The ellipse captured the general shape of the cross-section, but did not account for finer morphological features. These finer features were analysed by subtracting the elliptical approximation of each cross-section (e) from the original cross-sectional data (R). The resulting residuals (r), represented the non-elliptical aspects of the stalk. Morphological patterns within the residuals were then decomposed using principal component analysis. These relationships are expressed mathematically as follows:

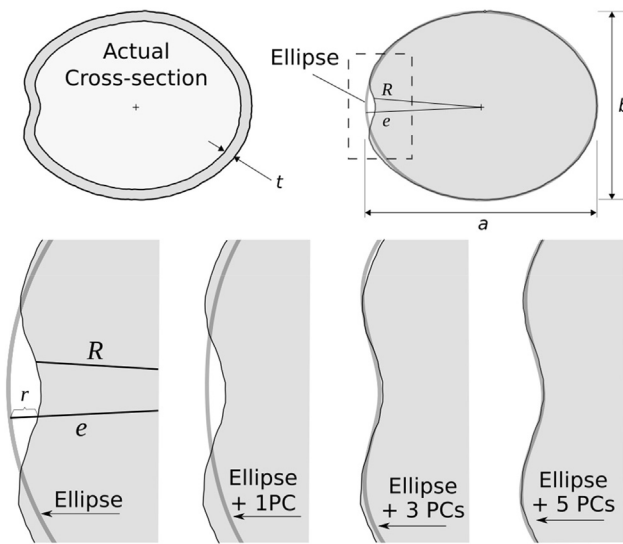


Fig. 2 – Top left: Illustration of an actual cross-section. **Top right:** cross-section and corresponding ellipse approximation with major and minor diameters (interior boundaries excluded for clarity). **Bottom:** enlarged views depicting geometric convergence to the true shape of the cross-section (shown in shaded grey) as additional principal components are included. The symbols R , e , and r , correspond to the symbols used in Eqs. 1 and 2, but with subscripts omitted for clarity.

$$R_{ik} = e_{ik} + r_{ik} \quad (1)$$

$$R_{ik} = e_{ik} + \sum_{j=1}^N P_{ij} s_{jk} + \varepsilon_{ikN} \quad (2)$$

In these equations, the index i refers to 360 angular sampling points (one per degree) while k refers to a specific stalk cross-section (12,740 in total, see section 2.4). The principal component decomposition is captured by the summation term where P_{ij} refers to the N principal components ($j = 1, 2, 3, \dots, N$), and s_{jk} refers to the corresponding set of scaling factors for each cross-section. Finally, ε_{ikN} represents the discrepancy between the geometric approximation and the actual stalk. When all principal components are included ($N = 360$), all ε_{ikN} terms are zero.

The number of possible parameters was reduced by modelling the geometry of the rind as a constant offset from the exterior boundary. This assumption has been shown to be both useful and accurate in prior studies (Robertson et al., 2017; Stubbs et al., 2019). The rind thickness of each cross-section was obtained by computing the average distance between the exterior and interior boundaries obtained during segmentation.

This geometric decomposition provided a very detailed approximation of the cross-sectional morphology of the maize stalk when using 5 principal components (see bottom right image in Fig. 2). Thus, the morphology of each cross-section was described by 3 ellipse parameters: major diameter (a), minor diameter (b), rind thickness (t), plus 0–5

principal components. Graphical depictions of various geometric models are provided in Fig. 2.

2.3. Loading cases and models

Four loading cases were used to assess the predictive accuracy of each geometric approximation. These loading cases are shown in Fig. 3 and include axial tension/compression; bending; transverse compression, and torsion. The transverse compression loading case used finite element modelling, while the other three loading cases relied upon analytic equations.

Torsion, tension/compression, and bending models all utilised a fixed length of 100 mm.

2.3.1. Analytic models: tension/compression, torsion and bending models

Two-tissue analytic models were used to compute structural responses for the axial, bending, and torsional loading cases. This required the numeric calculation of the cross-sectional area, area moment of inertia, and polar moment of inertia for each cross-sectional approximation. The response was then evaluated using the analytic equations listed in Table 1. As our study focuses on relative changes between the actual and approximated geometries, the length factor cancelled out of all results and thus had no influence on the corresponding results.

2.3.2. Material properties

Maize tissues are well-approximated as linearly elastic, transversely isotropic (Stubbs et al., 2019, 2018). Transversely isotropic materials require 5 independent material properties (Cook et al., 2008). In general, an application of this material model to the maize stalk would require 10 independent material properties. However, because here we are only interested in a two-dimensional cross-section, the structural models used in this study were each dependent upon the two material properties activated by each loading case. The material property distributions used in this study are listed in Table 1.

2.3.3. Transverse compression models

A finite-element modelling approach was used to analyse the response of the maize cross-section to transverse compression. Models were created in ABAQUS/CAE 2017 by specifying the internal and external boundaries of rind and pith regions. Finite-element meshes were generated using the Medial Axis Algorithm (Simulia, 2016). Adequate element sizes were determined from a mesh convergence study. An example of the mesh is provided in Fig. 4 below.

As shown in Fig. 4, the major axis of each cross-section was oriented in the horizontal direction and loading was applied in the vertical direction, along the minor axis. A fixed boundary condition was applied along the bottom of each cross-section. A displacement of 0.005 mm was applied directly opposite to the fixed boundary condition. The outcome of each simulation was the transverse stiffness (i.e. force/deformation slope) of the model to transverse compression.

The transverse compression model used in this study has been previously validated through comparisons with physical

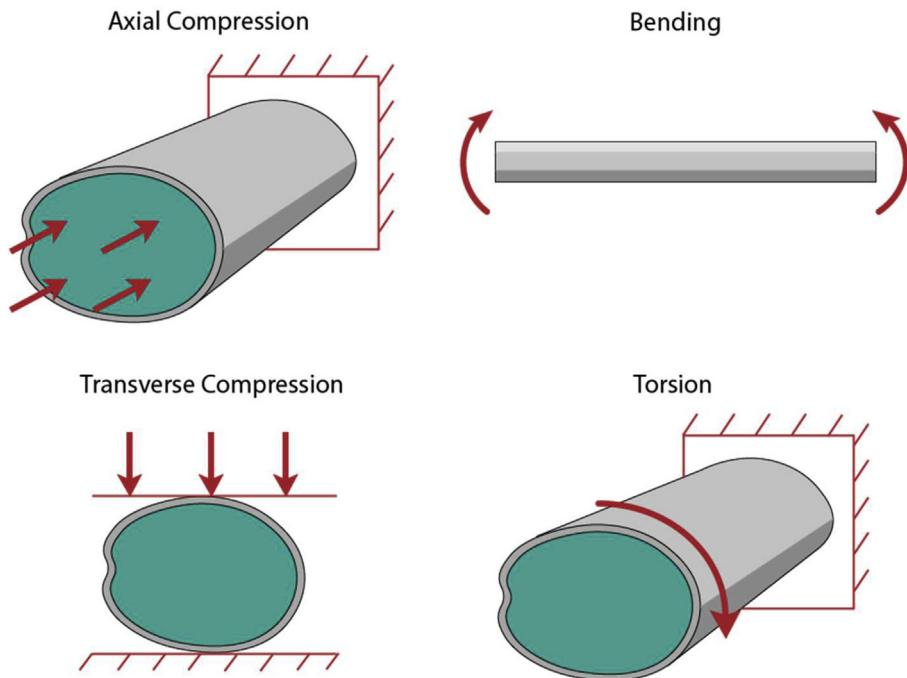


Figure 3 – The prismatic models and loading cases analysed in this study.

specimens (Stubbs et al., 2019). Additional details on the validation of this model are available in a graduate thesis (Larson, 2020).

2.4. Cross-sectional sampling

Two sampling groups were used in this study. First, CT cross-sections used in this study were drawn from thirteen sample points ranging from 40 mm above the node to 40 mm below the node. This set of cross-sections is referred to as Group 1 (see Fig. 5). As seen in this figure, more points were sampled near the node in order to provide higher fidelity where the maize stalk fails most frequently (Robertson et al., 2015). Group 1 included 12,740 unique cross-sectional images: thirteen sample points for each of the 980 stalks in the data set. Group 2 consisted of 70 cross-sections sampled from 5 of the 13 cross-sections of Group 1. This resulted in a total of 350 stalks in Group 1. Figure 5 illustrates the scan region, the associated sampling points, and provides representative cross-sectional images.

2.5. Assessment

2.5.1. Assessing geometric fidelity

For each cross-section in Group 1, a series of approximate geometries was created: these started with an ellipse to which principal components were successively added until all 360 principal components were included (at which point an exact recreation of the original geometry was obtained). The radial error between each approximation and the corresponding original geometry is given by the term ε_{ikN} (see Eq. (2)). To allow comparisons of errors within and between cross-sections, these error values were normalised by dividing each individual error value by the minor diameter of the

associated cross-section (b_k , see Eq. (4)). This choice for the denominator ensures that all errors values are conservative. The distributions of relative error were used to assess geometric fidelity of the various approximations.

$$\text{Percent Geometric Error} = \frac{\varepsilon_{ikN}}{b_k} \quad (3)$$

2.5.2. Assessing structural response

A similar approach was used to assess the predictive accuracy of various geometric approximations. The structural assessment used the 350 Group 2 cross-sections shown in Fig. 5, as these are located in the region where failure most commonly occurs (Robertson et al., 2015). For each cross-section and loading case, a reference model was created from the original interior and exterior boundaries. A corresponding elliptical approximation model was then created. Next, principal components were added to the ellipse in sequence to obtain various geometric approximations. Comparisons between the force/deformation response of the reference model and each of these approximate models were used to assess the accuracy of each approximate model, as shown in Eq. (5) below.

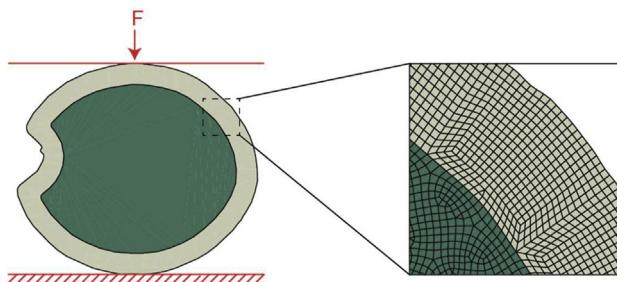
$$\text{Percent Response Error} = \frac{(F/\delta)_{approx} - (F/\delta)_{ref}}{(F/\delta)_{ref}} \quad (4)$$

where F/δ represents the force/deformation response of the model (torque/angular deformation in the case of torsion), and the subscripts “approx” and “ref” refer to the approximate and reference models, respectively.

A set of 350 reference models were created for each loading case. Each reference model was compared to a series of 9 approximate models under the same loading cases. Due to the higher cost of generating and analysing finite element models, only 6 approximate models were used for the transverse

Table 1 – Structural models and material properties used in each loading case.

| Loading Case | Structural Model | Material Properties | Property Sources |
|------------------------|--|---|---|
| Axial | $K_{\text{axial}} = \frac{E_{\text{pith}} A_{\text{pith}} + E_{\text{rind}} A_{\text{rind}}}{L}$ (3) | $E_{\text{rind}, k} = 11 \pm 2 \text{ GPa}$ $E_{\text{pith}, k} = 0.33 \pm 0.06 \text{ GPa}$ | (Al-Zube et al., 2018, 2017) |
| Bending | $K_{\text{bending}} = \frac{48(E_{\text{pith}} I_{\text{pith}} + E_{\text{rind}} I_{\text{rind}})}{L^3}$ (4) | | |
| Torsion | $K_{\text{torsion}} = \frac{G_{\text{pith}} J_{\text{pith}} + G_{\text{rind}} J_{\text{rind}}}{L}$ (5) | $G_{\text{rind}, k} = 8 \pm 2 \text{ GPa}$ $G_{\text{pith}, k} = 0.25 \pm 0.06 \text{ GPa}$ | No measurements currently available. Estimated from wood literature (Green et al., 1999) |
| Transverse Compression | Finite element model | $E_{\text{rind}, k} = 8.07 \pm 3.3 \text{ GPa}$ $E_{\text{pith}, k} = 0.259 \pm 0.1 \text{ GPa}$ | (Stubbs et al., 2019) |

**Fig. 4 – Schematic diagram of loading conditions and the finite element mesh used to compute the response of the transverse compression loading case.**

compression loading case. This experimental design is outlined in Table 1 below.

2.6. Sensitivity analysis

To further quantify the influence of each model parameter, a series of local sensitivity analyses were performed. A unitless normalised sensitivity approach was used since this approach allows comparisons across input/output pairs of different units (Robertson, Zañartu, & Cook, 2016). The local sensitivity analysis was performed by changing one parameter at a time by 10% and then computing the normalised sensitivity as a finite difference numerical derivative, as shown here:

$$S = \frac{(y_{\text{new}} - y_{\text{ref}}) / y_{\text{ref}}}{(x_{\text{new}} - x_{\text{ref}}) / x_{\text{ref}}} \quad (5)$$

In this equation, x_{ref} and y_{ref} represent the input and response of the reference case while x_{new} and y_{new} represent the input and response values from the modified case. The sensitivity can be interpreted as the percent change in output divided by the percent change in input.

3. Results

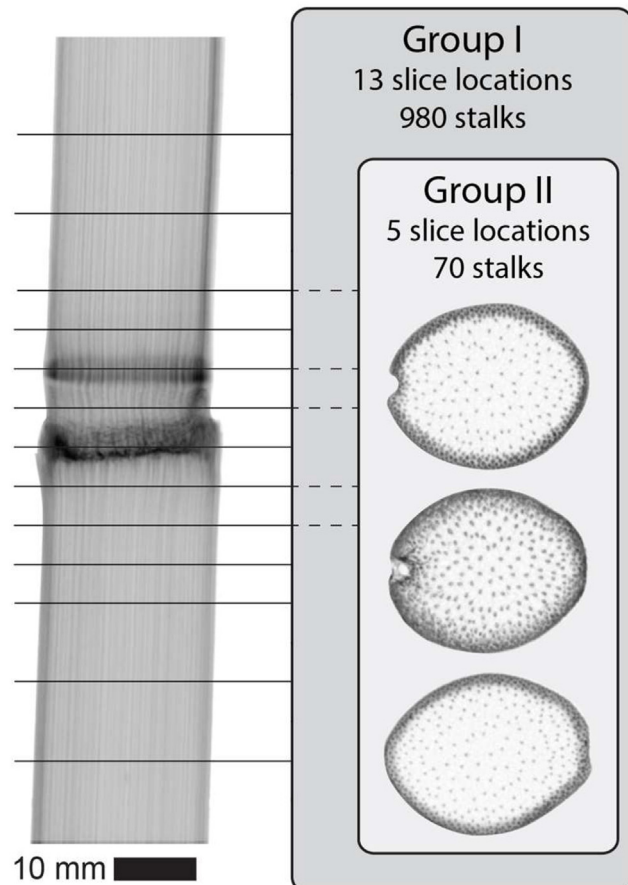
3.1. Components of the geometric decomposition

The components of geometric decomposition are shown in Fig. 6. In each panel, the shaded regions depict the distribution of underlying data, with darker regions indicating higher data density. The first principal component primarily captures data variation corresponding to the tall peaked region (the “ear groove”). Subsequent principal components capture

additional features of the underlying data. While Fig. 5 is informative, animated plots are much more effective for visualising the individual principal components. Animated GIF (Graphics Interchange Format) representations of each of the 5 principal components are therefore provided as [supplementary figures](#).

3.2. Geometric fidelity

The geometric decomposition approach described in the methods section allowed the original geometry of each cross-section to be approximated using an ellipse plus principal components. Figure 7 shows the distribution of error values which are obtained as an increasing number of principal

**Fig. 5 – Illustration of the CT slice locations and group sampling used in this study**

components are included in the model. As shown in Fig. 7, error values reach 0 as all 360 principal components are included. The ellipse alone captures approximately 90% of the cross-sectional shape. Adding one principal component reduces the error to below 5%. With 5 principal components included, the vast majority of error values (95%) have magnitudes less than 1.5%.

3.3. Structural response

Results above suggest that high geometric accuracy can be obtained with relatively few geometric parameters. Next, we examined the relationships between geometry and mechanical response to loading cases using just the first several principal components. Overall, the response of approximate models was found to be highly accurate, even when using approximated models. The charts of Fig. 8 depict the error distributions for various geometric approximations for each of the four loading cases. In these charts, relative error was defined as the percent difference in structural response between the approximate model and the corresponding model based on the original cross-section.

As seen in Fig. 8, as additional principal components were added to the ellipse, the mechanical response quickly approached the response obtained when using the original cross-section. The ellipse alone provided better than 95% accuracy (errors less than 5%) for the axial, bending, and transverse compression cases. For the torsional loading, the ellipse

alone was 90% accurate. In each case, the addition of principal components progressively reduced error, with error levels within 1% at 5 principal components for axial, bending, and transverse loads, and within 1% after 6 principal components for torsional loads.

3.4. Sensitivity analysis

The influence of each model parameter on the four types of mechanical response was quantified by computing normalised sensitivities. This approach normalised all results, thus facilitating comparisons between parameters as well as across loading cases. The output of interest was the force/deformation stiffness of each loading case. Sensitivity results are shown in terms of absolute values with negative sensitivities indicated by a (–) symbol. These results are shown in Fig. 9. Note that each panel of Fig. 9 is split into three parameter groups: ellipse parameters, material properties, and principal components.

The most consistent finding was that principal components had minimal influence on the structural responses. The greatest influence of principal components was for the torsion loading. This is because the polar moment of inertia is very sensitive to minor changes in the geometry of the outer rind tissue. However, even for the torsional case, most sensitivity values were below 5%. This indicates that a 10% increase in the principal component scaling factor would result in only a 0.5% change in the response. In contrast, a 10% increase in the

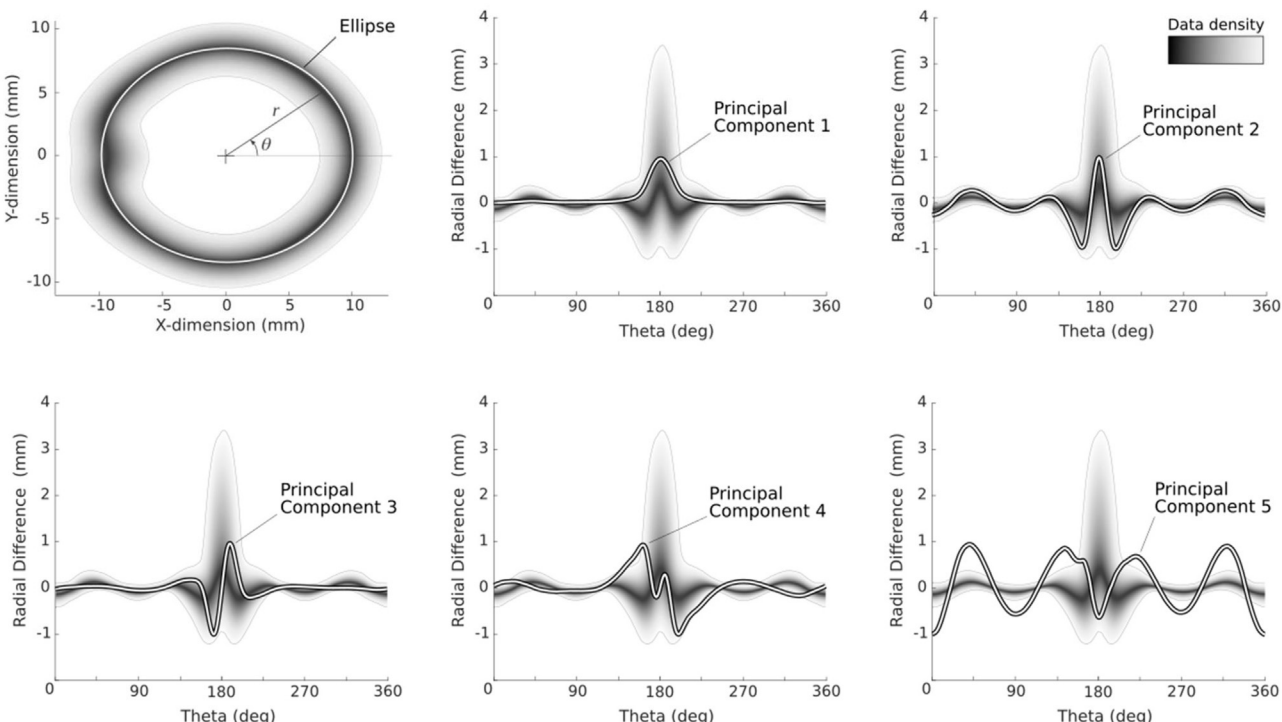


Fig. 6 – Individual geometric components (white lines) superimposed over data distributions (shaded). The top left panel shows the distributions of the maize stalk cross-sections with the mean ellipse superimposed over the data distribution. The remaining panels show the 5 principal components superimposed over the ellipse-subtracted data (polar form, plotted in rectangular coordinates). The outer limits of the shaded regions are at 95% confidence levels. Animations of the principal components are available in [supplementary figures](#).

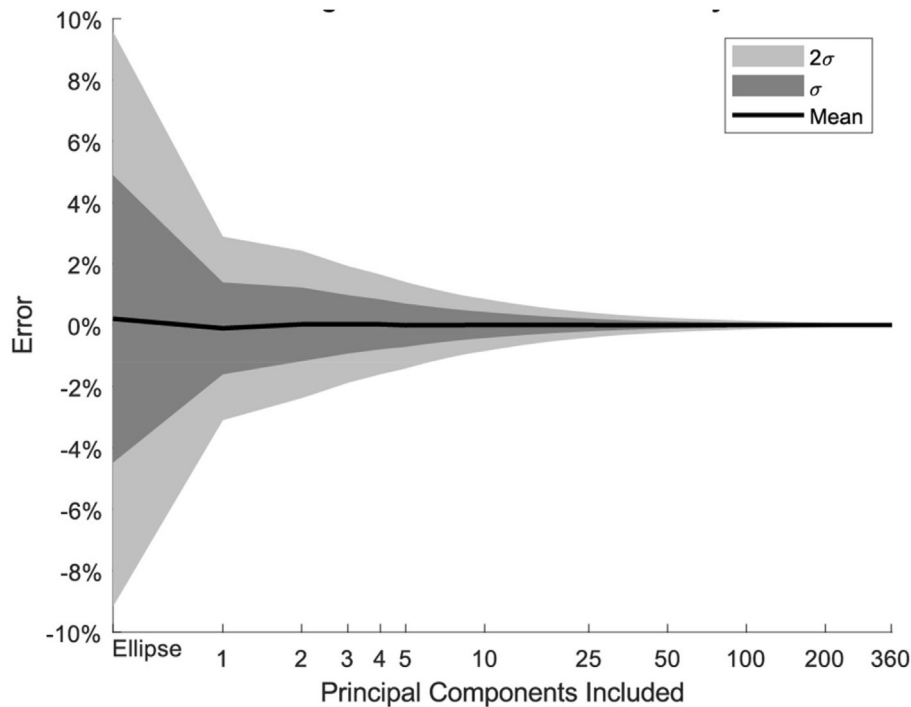


Fig. 7 – The convergence pattern of geometric errors. Relative error was defined as the difference between true and approximated geometry, normalised by the minor diameter of each cross section (see Eq. (3)).

major diameter (a) would increase the torsional stiffness by approximately 18%.

Across all loading cases, the most influential parameters belonged to either the ellipse or mechanical tissue properties groups. For axial, bending, and torsional loading, the influence of the rind modulus was many times more influential than the modulus of the pith tissue. However in transverse stiffness, the pith tissue was more influential than the modulus of the rind. In fact, one important role of the pith is to allow the maize stalk to resist cross-sectional ovalisation, thereby increasing the critical buckling load (Karam & Gibson, 1994).

As expected, the influence of geometric parameters (a , b , and t) varies according to the different loading cases. For example, bending stiffness is most sensitive to the minor axis (b), while torsion is highly sensitive to both radius values (a and b), etc. The rind thickness was found to have the highest influence on transverse stiffness, with a mean sensitivity of 97%. This is approximately the same as a 1:1 influence. The next most influential parameters were major diameter and the Young's Modulus of the pith tissue. The Young's Modulus of the rind and the minor diameter had relatively low sensitivity values (0.3 and -0.08, respectively). Transverse compression exhibited notably broader distributions than the other loading case. This was found to be caused by strong nonlinear relationships between the morphology of the cross-section and the resulting sensitivities.

3.5. Application case study

The decomposition method described above can be applied to any maize cross-section. This was performed using a

photograph of a maize stalk cross-section. The results are shown in Fig. 10. The exterior boundary of a maize stalk was segmented (upper left panel of Fig. 10). This data was then fit with an ellipse and the residuals were decomposed using the principal components from Fig. 6. Decomposition was performed using a least-squares approach. The principal components were used as basis vectors and the least-squares approach solved for the scaling factor of each principal component that best approximated the residuals for this particular stalk. Additional details on this process are found in the supplementary information that accompanies this paper. The results are shown in Fig. 10 along with geometric variation of the three ellipse parameters and the first two principal components.

As seen in Fig. 10, the first principal component primarily affects the depth of the ear groove, while the second principal component accentuates the profile of the ear groove. This approach provides a convenient method for both decomposing and manipulating the shape of the maize stalk cross-section. The method does not require a separate principal component analysis, only the principal components themselves (which are available as [supplementary data](#)).

4. Discussion

4.1. The ellipse as an efficient parameterised model

The purposes of this study were to (a) develop a parameterised two-dimensional model of the maize cross-section and (b) test the relationships between level of geometric detail and model

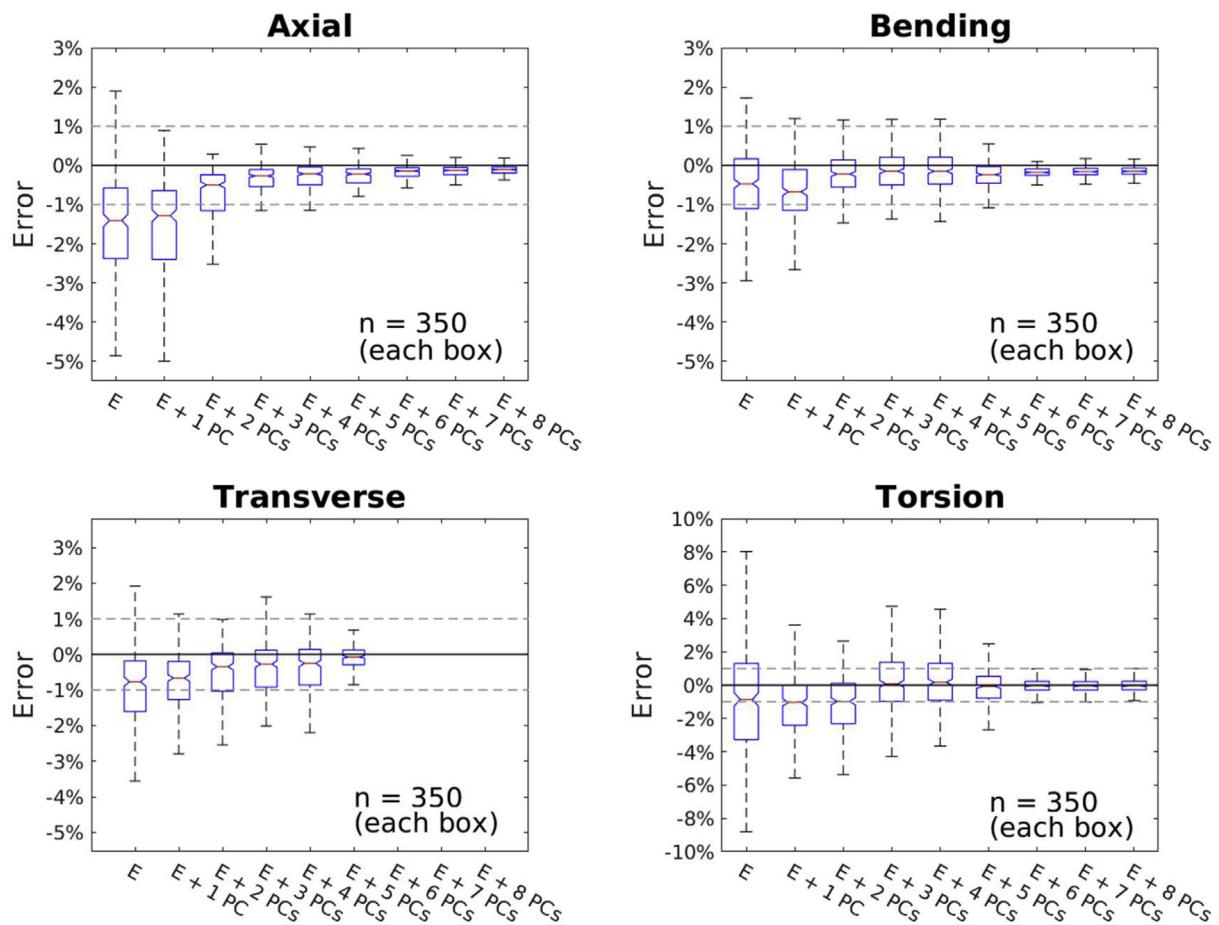


Fig. 8 – Convergence patterns showing the distributions of relative errors obtained with models consisting of various numbers of geometric components. Error is defined as the percentage difference between the approximate model and the original maize cross-section.

accuracy. This work represents an important first step towards a full parameterised three-dimensional model. This is significant for two reasons. First, current models rely on specimen-specific geometry, which cannot be readily manipulated (Stubbs et al., 2022; Von Forell et al., 2015). Second, parameterised models enable a much greater range of future and more advanced analyses such as optimisation of the maize stalk morphology, sensitivity analyses, etc..

The results shown in Fig. 7 indicate that the simple ellipse can be used to approximate the geometry itself with geometric errors typically less than 10%. The ellipse also provided remarkably accurate estimations of structural stiffness in axial, bending, and transverse loading cases (Fig. 8). For each of these cases, the ellipse alone was able to predict structural stiffness with errors of less than 5%. For the case of torsion, the ellipse exhibited structural discrepancies of less than 10%. This conclusion is further reinforced by the results of Fig. 9, which show that the ellipse parameters exert far more influence on the structural response than any of the principal components. Finally, these results are in agreement with the prior empirical observations which suggested that the ellipse provides an effective approximation of the maize cross-section under bending loads (Robertson et al., 2017).

It has been suggested that tissue weaknesses associated with low-lignin maize varieties could be offset by targeted changes to stalk morphology, thus enabling new varieties that produce high grain yield and having stover biomass that is readily converted to biofuel (Robertson et al., 2022; Von Forell et al., 2015). Parameterised engineering models of the maize stalk could be used along with optimisation techniques to determine what types of changes may be most beneficial in reaching this goal. Since the ellipse is defined by three parameters (major diameter, minor diameter, and rind thickness), cross-sectional models of simple loading cases can be described by just 5 parameters: 3 for the ellipse, and 2 for the tissue. This provides a very compact and convenient way of parameterizing the cross-section while still providing high levels of predictive accuracy.

The small number of cross-sectional parameters may be very useful in future research aimed at a three-dimensional parameterisation of the maize stalk geometry. Such models are computationally expensive, which makes a simultaneous study of longitudinal and cross-sectional features impractical. The cross-sectional models developed in this study will allow future studies to focus purely on the longitudinal patterns inherent in maize stalk morphology.

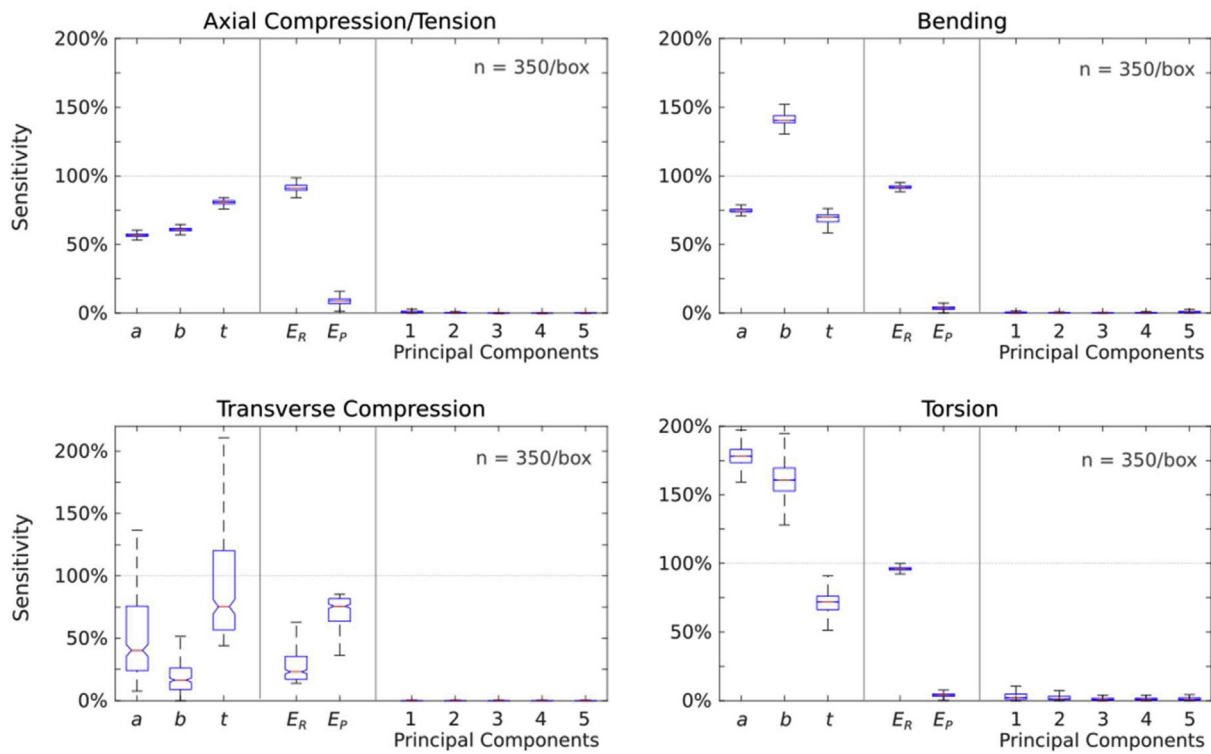


Fig. 9 – Normalised sensitivity results for each loading case. Horizontal lines within each box represent 25th, 50th, and 75th percentiles. Whiskers tips indicate 95% coverage for each distribution

The ellipse model is the recommended starting point, but principal components can always be added to the ellipse to attain any level of specified accuracy. There are several powerful advantages to using a principal component approach. Firstly, as seen above, it provides a decomposition in which a small number of components can be used to create highly accurate approximations. Secondly, if all principal components are included then an exact reconstruction of the original data is obtained (Jackson, 2005). Thirdly, principal components are mutually orthogonal. Thus, each principal component captures a distinct pattern, as defined by the distribution of variance in the original data (*ibid*). Orthogonality has significant implications in optimization since variation in one principal component is guaranteed to be independent of variation in the other principal components. Finally, the application of this method does not require a separate principal component analysis and can thus be readily applied to any stalk.

4.2. Limitations

Firstly, we acknowledge that the simplified loading conditions used in this study differ from those experienced by real stalks. Simplified structural models were intentionally used in this study because they enabled a comprehensive evaluation of many different model configurations (~27,000 different models, see Table 2). Although simple models were used, each simple loading model exhibited a similar pattern in which the ellipse provided a favourable balance between accuracy and model complexity. The principle of linear superposition indicates that (at least for small deformations) structural

stresses are additive and do not interact. Thus, although the loading cases used in this study are simplistic, they represent important components of more complex loading situations.

Transverse ovalisation was modelled in this study by applying a transverse compressional load to two-dimensional models of the maize cross-section (Fig. 4). This approach was chosen because (a) it builds upon previously validated cross-sectional models of the maize cross-section (Stubbs et al., 2019), and (b) it allows a means of quantifying resistance to transverse deformation using a two-dimensional model. As stated previously, localised Brazier buckling is determined by the amount of transverse ovalisation (Leblanc et al., 2015; Schugasser & Witztum, 1992). However ovalisation that occurs during bending is more complex than the situation examined in this study. In other words, we acknowledge that transverse deformation is a simplification and is therefore not necessarily predictive of true ovalisation.

The most significant geometric limitation in this study is the assumption of constant rind thickness. An alternative (and more accurate) approach would be to decompose the interior boundary of the maize stalk using a separate ellipse and additional principal components. This approach was not used because it would have doubled the total number of geometric parameters. But it would not have significantly increased predictive accuracy (in most cases, the ellipse plus 5 principal components produced models with errors less than $\pm 1\%$).

Additional (but relatively minor) limitations include the use of several simplifying assumptions. For example, tissues were modelled as transversely isotropic and linear elastic. The plane-stress assumption was invoked in transverse

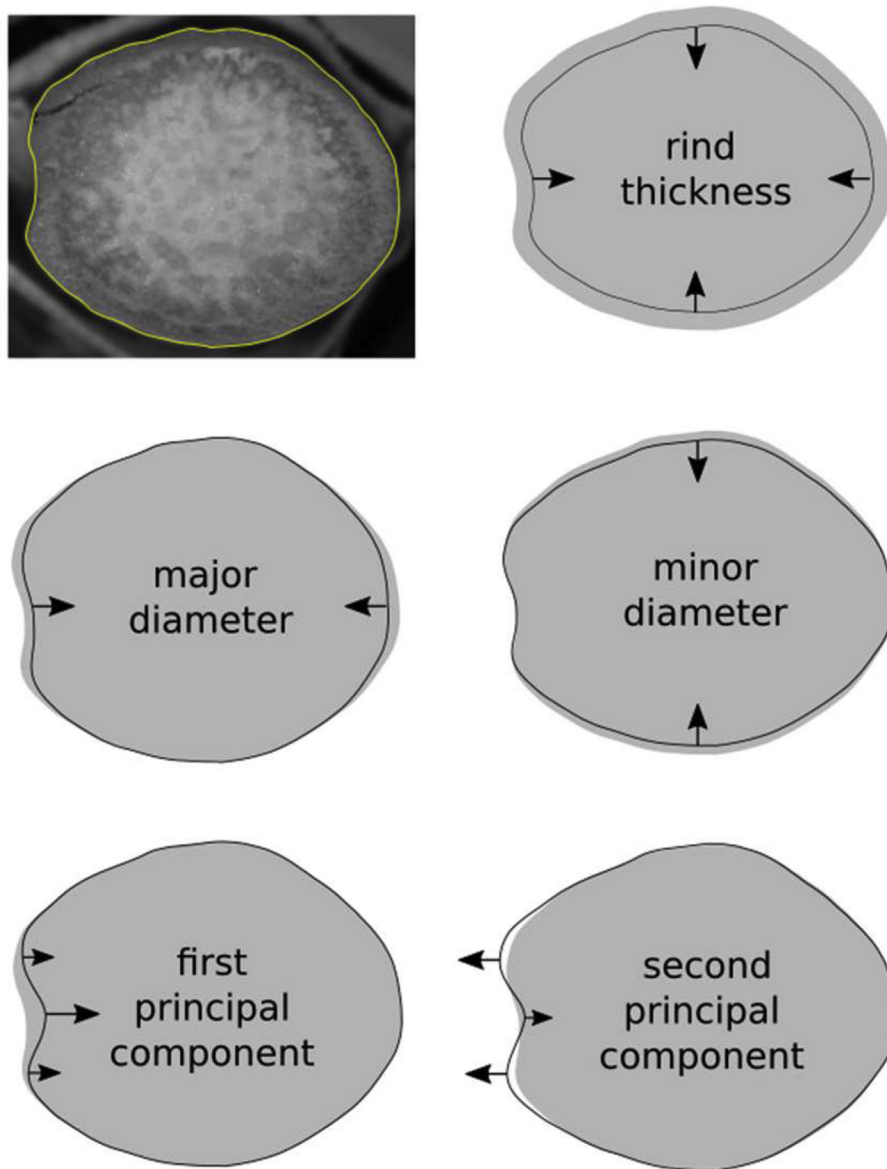


Fig. 10 – The application of geometric decomposition and parametric variation to an arbitrary maize stalk cross-section. Top left: Photograph and exterior boundary of the original cross-section. The remaining 5 panels show the original cross-sectional shape in grey with parametric modification of the parametric model shown as black lines. The rind thickness was omitted from these panels for the sake of image simplicity/clarity. Arrows emphasize the major directions of variation.

compression. Maize tissue properties were assumed constant within each tissue region, rather than having a stiffness gradient (Stubbs, Larson, & Cook, 2020). All simulations were static in nature and did not include any dynamic effects. However, since the primary goal was to develop a useful and accurate geometric model, not to investigate the actual mechanics of transverse ovalisation, we believe that each of these assumptions are justified and appropriate.

4.3. Limitations in context

The limitations listed above should be evaluated within the context and purpose of this study. While many studies seek to predict behaviour, this study was conducted to develop a

parsimonious cross-sectional model of maize stalk geometry. For this purpose, simple models served as efficient mechanistic test cases, while also enabling the evaluation of many more cross-sections and geometric variability than would have been possible using more complex models such as three-dimensional solid models. This approach is appropriate because there are currently very few modelling studies that have focused on this system. The results of this study support the idea that a simple ellipse provides an excellent approximation of the maize stalk cross-section. This assumption could drastically simplify future modelling efforts. However, we recognise that future studies will need to confirm that the ellipse assumption is equally predictive in more complex loading conditions.

Table 2 – Experimental design overview showing the number of reference models, number of geometric approximations, and the number of models in the geometric approximation study and sensitivity analysis study.

| Loading Case | Reference Models | Geometric approximations | Geometric approximation models | Sensitivity analysis models | Total models analysed |
|---------------------------|------------------|--------------------------|--------------------------------|-----------------------------|-----------------------|
| Axial tension/compression | 350 | X | 9 | = | 3,150 |
| Bending | 350 | X | 9 | = | 3,150 |
| Transverse compression | 350 | X | 6 | = | 2,100 |
| Torsion | 350 | x | 9 | = | 3,150 |
| | | | | | Grand Total |
| | | | | | 26,950 |

5. Conclusions

In this study, the cross-section geometry of the maize stalk was decomposed into an ellipse plus a series of geometric patterns (principal components). The resulting geometric model is advantageous because it provides both geometric control and varying levels of geometric fidelity. We used the parameterised model to rigorously explore the relationship between cross-sectional morphology and predictive model accuracy. The ellipse was found to provide a simple yet effective model of the maize stalk cross-section. The ellipse alone captured approximately 90% of the overall shape of the cross-section. Structural models based on the ellipse alone exhibited errors that were typically less than 5%, indicating that the simple ellipse provides remarkably accurate approximations of actual responses. The components of the ellipse were also found to be far more influential on structural outcomes than the principal components. In general, principal components had minimal influence on structural outcomes. By adding principal components, the discrepancy between the response of the original cross-section and the approximate model can be reduced to any desired level of accuracy.

These conclusions should be interpreted with simplifying assumptions in mind. This study utilised simple loading conditions which differ somewhat from the more complex loading conditions that maize stalks experience in the field. Future studies will be needed to confirm the accuracy and validity of the ellipse assumption in scenarios that differ from those used in this study.

In conclusion, the ellipse assumption effectively simplifies the maize cross-section by providing an acceptable level of accuracy across four different loading cases while requiring just three geometric parameters: major diameter, minor diameter, and rind thickness. In addition, if more geometric detail is needed, the models presented in this study allow for any desired degree of model fidelity. By providing a parameterisation of the maize cross-section, and quantifying the relationship between cross-sectional shape and model accuracy, this study provides a foundation for future research aimed at efficiently performing optimisation and sensitivity analyses of the maize stalks.

Authors' contributions

All authors were involved in the study and preparation of the manuscript. The material within has not been and will not be submitted for publication elsewhere.

Consent for publication

Not applicable.

Availability of data and materials

The datasets used and/or analysed during the current study are available from the corresponding author on reasonable request.

Funding

This work was supported by an NSF CAREER Award, #2046669 and by the Ira Fulton College of Engineering, Brigham Young University.

Declaration of competing interest

The authors declare that they have no known competing financial interests or personal relationships that could have appeared to influence the work reported in this paper.

Appendix A. Supplementary data

Supplementary data to this article can be found online at <https://doi.org/10.1016/j.biosystemseng.2022.03.010>.

REFERENCES

Ahmad, I., Kamran, M., Ali, S., Bilegjargal, B., Cai, T., Ahmad, S., Meng, X., Su, W., Liu, T., & Han, Q. (2018). Uniconazole application strategies to improve lignin biosynthesis, lodging resistance and production of maize in semiarid regions. *Field Crops Research*, 222, 66–77. <https://doi.org/10.1016/j.fcr.2018.03.015>

Al-Zube, L. A., Robertson, D. J., Edwards, J. N., Sun, W. H., & Cook, D. D. (2017). Measuring the compressive modulus of elasticity of pith-filled plant stems. *Plant Methods*, 13, 1–9. <https://doi.org/10.1186/s13007-017-0250-y>

Al-Zube, L., Sun, W., Robertson, D., & Cook, D. (2018). The elastic modulus for maize stems. *Plant Methods*, 14(1), 1–12. <https://doi.org/10.1186/s13007-018-0279-6>

Besnault, B., Lavaste, F., Guillemot, H., Robin, S., & Le Coz, J.-Y. (1998). A parametric finite element model of the human pelvis.

SAE Transactions, 107, 2680–2694. <https://www.jstor.org/stable/44741230>.

Cook, D. D., de la Chapelle, W., Lin, T.-C., Lee, S. Y., Sun, W., & Robertson, D. J. (2019). Darling: A device for assessing resistance to lodging in grain crops. *Plant Methods*, 15(1), 102. <https://doi.org/10.1186/s13007-019-0488-7>

Cook, D., Julias, M., & Nauman, E. (2014). Biological variability in biomechanical engineering research: Significance and meta-analysis of current modeling practices. *Journal of Biomechanics*, 47(6), 1241–1250. <https://doi.org/10.1016/j.jbiomech.2014.01.040>

Cook, D. D., Nauman, E., & Mongeau, L. (2008). Reducing the number of vocal fold mechanical tissue properties: Evaluation of the incompressibility and planar displacement assumptions. *Journal of the Acoustical Society of America*, 124(6), 3888–3896. <https://doi.org/10.1121/1.2996300>

Davis, S. M., & Crane, P. L. (1976). Recurrent selection for rind thickness in maize and its relationship with yield, lodging, and other plant characteristics. *Crop Science*, 16, 53–55.

Devey, M. E., & Russell, W. A. (1983). Evaluation of recurrent selection for stalk quality in a maize cultivar and effects on other agronomic traits [Diplodia maydis, Zea mays, stalk rot]. *Iowa State Journal of Research*, 58(2), 207–219.

Duvick, D. N. (2005). The contribution of breeding to yield advances in maize (Zea mays L.). *Advances in Agronomy*, 86, 83–145. [https://doi.org/10.1016/S0065-2113\(05\)86002-X](https://doi.org/10.1016/S0065-2113(05)86002-X)

Erndwein, L., Cook, D. D., Robertson, D. J., & Sparks, E. E. (2020). Field-based mechanical phenotyping of cereal crops to assess lodging resistance. *Applications in Plant Sciences*, 8(8), Article e11382. <https://doi.org/10.1002/aps3.11382>

Flint-Garcia, S. A., Jampatong, C., Darrah, L. L., & McMullen, M. D. (2003). Quantitative trait locus analysis of stalk strength in four maize populations. *Crop Science*, 43, 13–22. <https://doi.org/10.2135/cropsci2003.0013>

Gomez, F. E., Muliana, A. H., Niklas, K. J., & Rooney, W. L. (2017). Identifying morphological and mechanical traits associated with stem lodging in bioenergy sorghum (sorghum bicolor). *Bioenergy Research*, 10, 635–647. <https://doi.org/10.1007/s12155-017-9826-7>

Gou, L., Huang, J., Zhang, B., Li, T., Sun, R., & Zhao, M. (2007). Effects of population density on stalk lodging resistant mechanism and agronomic characteristics of maize. <https://europepmc.org/article/cba/646421>.

Green, D. W., Winandy, J. E., & Kretschmann, D. E. (1999). Mechanical properties of wood. In *Wood handbook: Wood as an engineering material*. Madison, WI: USDA Forest Service, Forest Products Laboratory, 1999. General technical report FPL; GTR-113: Pages 4.1-4.45, 113.

Guo, Q., Chen, R., Ma, L., Sun, H., Weng, M., Li, S., & Hu, J. (2019). Classification of corn stalk lodging resistance using equivalent forces combined with SVD Algorithm. *Applied Sciences*, 9(4), 640. <https://doi.org/10.3390/app9040640>

Hondroyianni, E., Papakosta, D. K., Gagianas, A. A., & Tsatsarelis, K. A. (2000). Corn stalk traits related to lodging resistance in two soils of differing salinity. *Maydica*, 45(2), 125–133.

Hu, H., Liu, W., Fu, Z., Homann, L., Technow, F., Wang, H., Song, C., Li, S., Melchinger, A. E., & Chen, S. (2013). QTL mapping of stalk bending strength in a recombinant inbred line maize population. *Theoretical and Applied Genetics*, 126(9), 2257–2266. <https://doi.org/10.1007/s00122-013-2132-7>

Jackson, J. E. (2005). *A user's guide to principal components*. John Wiley & Sons.

Karam, G. N., & Gibson, L. J. (1994). Biomimicking of animal quills and plant stems: Natural cylindrical shells with foam cores. *Materials Science and Engineering: C*, 2(1), 113–132. [https://doi.org/10.1016/0928-4931\(94\)90039-6](https://doi.org/10.1016/0928-4931(94)90039-6)

Klein, K. F., Hu, J., Reed, M. P., Hoff, C. N., & Rupp, J. D. (2015). Development and validation of statistical models of femur geometry for use with parametric finite element models. *Annals of Biomedical Engineering*, 43(10), 2503–2514. <https://doi.org/10.1007/s10439-015-1307-6>

Larson, R. (2020). Development of a parameterised model of transverse maize (Zea mays L.) stalk morphology. Brigham Young University. <https://www.proquest.com/docview/2551170257>.

Lawlor, D. A., Tilling, K., & Davey Smith, G. (2016). Triangulation in aetiological epidemiology. *International Journal of Epidemiology*, 45(6), 1866–1886. <https://doi.org/10.1093/ije/dyw314>

Leblanc, T., Vanmaercke, S., Ramon, H., & Saeys, W. (2015). Mechanical analysis of the bending behaviour of plant stems. *Biosystems Engineering*, 129, 87–99. <https://doi.org/10.1016/j.biosystemseng.2014.09.016>

Manga-Robles, A., Santiago, R., Malvar, R. A., Moreno-González, V., Fornalé, S., López, I., Centeno, M. L., Acebes, J. L., Álvarez, J. M., & Caparros-Ruiz, D. (2021). Elucidating compositional factors of maize cell walls contributing to stalk strength and lodging resistance. *Plant Science*, 307, 110882. <https://doi.org/10.1016/j.plantsci.2021.110882>

Maurel, N., Lavaste, F., & Skalli, W. (1997). A three-dimensional parameterised finite element model of the lower cervical spine, study of the influence of the posterior articular facets. *Journal of Biomechanics*, 30(9), 921–931. [https://doi.org/10.1016/S0021-9290\(97\)00056-0](https://doi.org/10.1016/S0021-9290(97)00056-0)

Ma, D., Xie, R., Liu, X., Niu, X., Hou, P., Wang, K., Lu, Y., & Li, S. (2014). Lodging-related stalk characteristics of maize varieties in China since the 1950s. *Crop Science*, 54(6), 2805. <https://doi.org/10.2135/cropsci2014.04.0301>

Nelson, N., Stubbs, C. J., Larson, R., & Cook, D. D. (2019). Measurement accuracy and uncertainty in plant biomechanics. *Journal of Experimental Botany*, 70(14), 3649–3658. <https://doi.org/10.1093/jxb/erz279>

Reneau, J. W., Khangura, R. S., Stager, A., Erndwein, L., Weldekidan, T., Cook, D. D., Dilkes, B. P., & Sparks, E. E. (2020). Maize brace roots provide stalk anchorage. *Plant Direct*, 4(11), Article e00284. <https://doi.org/10.1002/pld3.284>

Robertson, D., Benton, Z., Kresovich, S., & Cook, D. (2022). Maize stalk lodging: Stalk architecture is a stronger predictor of stalk bending strength than chemical composition (accepted for publication) *Biosystems Engineering*. Submitted for publication.

Robertson, D. J., Julias, M., Gardunia, B. W., Barten, T., & Cook, D. D. (2015). Corn stalk lodging: A forensic engineering approach provides insights into failure patterns and mechanisms. *Crop Science*, 55(6), 2833–2841. <https://doi.org/10.2135/cropsci2015.01.0010>

Robertson, D. J., Julias, M., Lee, S. Y., & Cook, D. D. (2017). Maize stalk lodging: Morphological determinants of stalk strength. *Crop Science*, 57(2), 926. <https://doi.org/10.2135/cropsci2016.07.0569>

Robertson, D. J., Lee, S. Y., Julias, M., & Cook, D. D. (2016a). Maize stalk lodging: Flexural stiffness predicts strength. *Crop Science*, 56(4), 1711. <https://doi.org/10.2135/cropsci2015.11.0665>

Robertson, D., Zañartu, M., & Cook, D. (2016b). Comprehensive, population-based sensitivity analysis of a two-mass vocal fold model. *PLoS One*, 11(2), Article e0148309. <https://doi.org/10.1371/journal.pone.0148309>

Saltelli, A., & Funtowicz, S. (2014). When all models are wrong. *Issues in Science & Technology*, 30(2), 79–85. <https://www.jstor.org/stable/43315849>

Schulgasser, K., & Witztum, A. (1992). On the strength, stiffness and stability of tubular plant stems and leaves. *Journal of Theoretical Biology*, 155(4), 497–515. [https://doi.org/10.1016/S0022-5193\(05\)80632-0](https://doi.org/10.1016/S0022-5193(05)80632-0)

Seegmiller, W. H., Graves, J., & Robertson, D. J. (2020). A novel rind puncture technique to measure rind thickness and diameter

in plant stalks. *Plant Methods*, 16(1), 44. <https://doi.org/10.1186/s13007-020-00587-4>

Sekhon, R. S., Joyner, C. N., Ackerman, A. J., McMahan, C. S., Cook, D. D., & Robertson, D. J. (2020). Stalk bending strength is strongly associated with maize stalk lodging incidence across multiple environments. *Field Crops Research*, 249, 107737. <https://doi.org/10.1016/j.fcr.2020.107737>

Sher, A., Khan, A., Cai, L. J., Ahmad, M. I., Ashraf, U., & Jamoro, S. A. (2017). Response of maize grown under high plant density; performance, issues and management-a critical review. *Adv. Crop Sci. Technol.*, 5(3), 1–8. <https://doi.org/10.4172/2329-8863.1000275>

Sigal, I. A., Yang, H., Roberts, M. D., & Downs, J. C. (2010). Morphing methods to parameterise specimen-specific finite element model geometries. *Journal of Biomechanics*, 43(2), 254–262. <https://doi.org/10.1016/j.jbiomech.2009.08.036>

Simulia, D. S. (2016). *ABAQUS analysis manual*. Providence, RI, USA.

Song, Y., Rui, Y., Bedane, G., & Li, J. (2016). Morphological characteristics of maize canopy development as affected by increased plant density. *PLoS One*, 11(4), Article e0154084. <https://doi.org/10.1371/journal.pone.0154084>

Stubbs, C. J., Baban, N. S., Robertson, D. J., Alzube, L., & Cook, D. D. (2018). Bending stress in plant stems: Models and assumptions. In *Plant biomechanics*. Springer. <https://doi.org/10.1007/978-3-319-79099-2>.

Stubbs, C., Larson, R., & Cook, D. D. (2020b). Mapping spatially distributed material properties in finite element models of plant tissue using computed tomography. *Biosystems Engineering*, 200, 391–399. <https://doi.org/10.1016/j.biosystemseng.2020.10.008>

Stubbs, C. J., Larson, R., & Cook, D. D. (2022). Maize stalk stiffness and strength are primarily determined by morphological factors. *Scientific Reports*, 12(1), 1–11. <https://doi.org/10.1038/s41598-021-04114-w>

Stubbs, C. J., McMahan, C., Seegmiller, W., Cook, D. D., & Robertson, D. J. (2020a). Integrated Puncture Score: Force–displacement weighted rind penetration tests improve stalk lodging resistance estimations in maize. *Plant Methods*, 16(1), 1–12. <https://doi.org/10.1186/s13007-020-00654-w>

Stubbs, C., Sun, W., & Cook, D. D. (2019). Measuring the transverse Young's modulus of maize rind and pith tissues. *Journal of Biomechanics*, 84, 113–120. <https://doi.org/10.1016/j.jbiomech.2018.12.028>

Sun, Q., Liu, X., Yang, J., Liu, W., Du, Q., Wang, H., Fu, C., & Li, W.-X. (2018). MicroRNA528 affects lodging resistance of maize by regulating lignin biosynthesis under nitrogen-luxury conditions. *Molecular Plant*, 11(6), 806–814. <https://doi.org/10.1016/j.molp.2018.03.013>

Tongdi, Q., Yaoming, L., & Jin, C. (2011). Experimental study on flexural mechanical properties of corn stalks. *International Conference on New Technology of Agricultural*, 130–134. <https://doi.org/10.1109/ICAE.2011.5943766>, 2011.

USDA. (2018). *World agricultural supply and demand estimates*. <https://www.usda.gov/oce/commodity-markets/wasde/historical-wasde-report-data>.

Von Forell, G., Robertson, D., Lee, S. Y., & Cook, D. D. (2015). Preventing lodging in bioenergy crops: A biomechanical analysis of maize stalks suggests a new approach. *Journal of Experimental Botany*, 66, 4367–4371. <https://doi.org/10.1093/jxb/erv108>

Weizbauer, R. A., & Cook, D. D. (2022). Cell wall mechanics: Some new twists. *Biophysical Journal*, 121(6), 865–868. <https://doi.org/10.1016/j.bpj.2022.02.017>

Wen, W., Gu, S., Xiao, B., Wang, C., Wang, J., Ma, L., Wang, Y., Lu, X., Yu, Z., & Zhang, Y. (2019). In situ evaluation of stalk lodging resistance for different maize (*Zea mays* L.) cultivars using a mobile wind machine. *Plant Methods*, 15(1), 1–16. <https://doi.org/10.1186/s13007-019-0481-1>

Willman, M. R., Below, F. E., Lambert, R. J., Howey, A. E., & Mies, D. W. (1987). Plant traits related to productivity of maize. I. Genetic variability, environmental variation, and correlation with grain yield and stalk lodging 1. *Crop Science*, 27(6), 1116–1121.

Zhang, Y., Liang, T., Chen, M., Zhang, Y., Wang, T., Lin, H., Rong, T., Zou, C., Liu, P., & Lee, M. (2019). Genetic dissection of stalk lodging-related traits using an IBM Syn10 DH population in maize across three environments (*Zea mays* L.). *Molecular Genetics and Genomics*, 294(5), 1277–1288. <https://doi.org/10.1007/s00438-019-01576-6>

Zhang, Q., Zhang, L., Evers, J., Werf, W. van der, Zhang, W., & Duan, L. (2014). Maize yield and quality in response to plant density and application of a novel plant growth regulator. *Field Crops Research*, 164, 82–89. <https://doi.org/10.1016/j.fcr.2014.06.006>